

*Short note***Does break-up affect  ${}^9\text{Be} + {}^{209}\text{Bi}$  fusion at the barrier?**

C. Signorini<sup>1</sup>, Z.H. Liu<sup>2,5</sup>, Z.C. Li<sup>1,5</sup>, K.E.G. Löbner<sup>3</sup>, L. Müller<sup>1</sup>, M. Ruan<sup>2</sup>, K. Rudolph<sup>3</sup>, F. Soramel<sup>4</sup>, C. Zotti<sup>3</sup>, A. Andrighetto<sup>1</sup>, L. Stroe<sup>1</sup>, A. Vitturi<sup>1</sup>, H.Q. Zhang<sup>5</sup>

<sup>1</sup> Physics Department of University and INFN, via Marzolo 8, I-35131 Padova, Italy

<sup>2</sup> INFN, Legnaro National Laboratories, Legnaro, Padova, Italy

<sup>3</sup> Sektion Physik, Ludwig-Maximilians-Universität München, D-85748 Garching, Germany

<sup>4</sup> Physics Department of University and INFN, via delle Scienze 208, I-33100 Udine, Italy

<sup>5</sup> China Institute of Atomic Energy, P.O.Box 275(10), Beijing 102413, P.R. of China

Received: 22 February 1999 / Revised version: 26 March 1999

Communicated by D. Schwalm

**Abstract.** The  ${}^9\text{Be} + {}^{209}\text{Bi}$  fusion cross sections were measured in the  $36.0 \text{ MeV} \leq E_{\text{lab}} \leq 50.0 \text{ MeV}$  range, down to 0.6 mb, with high accuracy via in-beam detection of the ground state  $\alpha$ -decay of the evaporation residues produced. The elastic scattering cross sections around  $150^\circ$  and  $135^\circ$  were also obtained with moderate angular resolution. The cross sections below the barrier are reproduced by coupled channel calculations which include only one break-up channel with a moderate strength and a phenomenological renormalization of the potential depth. These simple calculations overestimate the cross sections above the barrier most likely due to the fact that the  ${}^9\text{Be}$  break-up process becomes much stronger. The barrier distributions extracted do not have evident break-up signature since they show one-barrier structure.

**PACS.** 25.70.Jj Fusion and fusion fission reactions

The influence of the break-up process (BU) on the fusion of two atomic nuclei at energies around the Coulomb barrier is being extensively investigated. The interest in this topic is primarily triggered by experiments now in progress and under consideration with radioactive beams of halo, loosely bound nuclei like  ${}^{11}\text{Be}$ ,  ${}^{11}\text{Li}$  ( $S_n=0.50 \text{ MeV}$  and  $S_{2n}=0.29 \text{ MeV}$  respectively). Such nuclei have binding energies much smaller than stable ones and consequently they are expected to break more easily in the fields of forces originating from the interaction with another nucleus. Indeed large BU cross sections, around 1 b, were measured [1–3] at energies well above the Coulomb barrier with  ${}^{11}\text{Be}$ ,  ${}^{11}\text{Li}$  and similar unstable nuclear beams. This has been reproduced by theoretical calculations [4,5] and is also expected at lower energies. A process with such a large cross section can influence the fusion around the Coulomb barrier; for this reason extensive theoretical calculations were done particularly in the subbarrier region for the system  ${}^{11}\text{Li}+{}^{208}\text{Pb}$  which presently constitutes one of the best combinations between halo beam and well stable nucleus. These calculations led to opposite predictions: enhancement [6] or hindrance [7,8] of the subbarrier fusion cross section.

In the region below the barrier the systems involving radioactive beams investigated up to now are:  ${}^{11,9}\text{Be} +$

${}^{209}\text{Bi}$  [9];  ${}^{17,19}\text{F} + {}^{208}\text{Pb}$  ( ${}^{17}\text{F}$  has  $S_p = 0.60 \text{ MeV}$ , no halo) [10] and  ${}^{11,9}\text{Be} + {}^{238}\text{U}$  [11], this last one has very low statistics. These experimental results do not give clear evidences of BU effects.

In the region immediately above the Coulomb barrier there are some evidences of BU effects in the fusion cross sections. The results [12] of the system  ${}^{11}\text{Be} + {}^{209}\text{Bi}$ , compared with  ${}^{10,9}\text{Be} + {}^{209}\text{Bi}$ , suggest that up to 25% of  ${}^{11}\text{Be}$  nuclei do not fuse as  ${}^{11}\text{Be}$  but as  ${}^{10}\text{Be}$  after undergoing nuclear BU. In addition, the results [13] from the systems  ${}^{6,7}\text{Li} + {}^9\text{Be}$ ,  ${}^{12}\text{C}$  ( ${}^6\text{Li}$  has  $S_\alpha = 1.47 \text{ MeV}$  and  ${}^9\text{Be}$   $S_n = 1.67 \text{ MeV}$ ) indicate a fusion cross section reduction of around 30% to 45%, assigned to the BU process, but some of these data were not confirmed in a later experiment [14].

All these experiments stimulated further investigations about possible effects of the BU process in the fusion one. Consequently it was decided to measure fusion cross sections with high accuracy also to derive the barrier distribution which constitutes a very sensitive test of how the fusion proceeds. The optimum projectiles like  ${}^{11}\text{Be}$ ,  ${}^{11}\text{Li}$ ,  ${}^8\text{B}$  had to be excluded because the present facilities are able to deliver beams with intensities around  $10^{+5} \text{ p/sec}$ , too weak for precision experiments. As a compromise the  ${}^9\text{Be} + {}^{209}\text{Bi}$  system, being well known to our experimental group [9,12], was chosen. The  ${}^9\text{Be}$  nucleus has one

of the lowest binding energies among the stable ones but still higher than an unstable one as  ${}^{11}\text{Be}$ . Consequently break-up phenomena should definitely be smaller, maybe of one magnitude order, but the beam intensities  $10^4$  to  $10^5$  times stronger allow high accuracy experiments which could give evidences for smaller effects, if existing.

The  ${}^9\text{Be}$  BU processes are in principle multiple since after a first step leading to  ${}^8\text{Be} + n$  a second one,  ${}^8\text{Be} \rightarrow 2\alpha$ , will automatically occur, the  ${}^8\text{Be}$  g.s. being unbound with  $T_{1/2} = 0.07$  fs; a third process where  ${}^9\text{Be}$  immediately breaks into  $n + \alpha + \alpha$  can also be hypothesized. Therefore we can have  ${}^8\text{Be}$  fusion and  $\alpha$  fusion/transfer reactions also followed by (mainly) neutron evaporation. In addition it should be considered that, in absence of any influence from external fields, the  ${}^8\text{Be}$  dissociation occurs in a time much longer than the reaction one. For these considerations the present work was focused upon the complete fusion of  ${}^{8,9}\text{Be}$  and not of  $\alpha$  particles since this second process should not be assigned to a pure fusion mechanism.

In the present work, which is a continuation of a previous one [12], the subbarrier fusion cross sections were measured in the low energy side down to one magnitude order smaller values and extended at higher energies up to 50 MeV. The elastic scattering cross sections, with low angular resolution, were also measured at two backward angles. From these data the barrier distributions were extracted. Partial results have already been reported [15].

The experiment was done with the  ${}^9\text{Be}$  beam delivered by the Munich Universities Tandem Van de Graaff accelerator. The energies covered were  $36.0 \text{ MeV} \leq E_{\text{lab}} \leq 38.5 \text{ MeV}$  in 0.5 MeV steps, 40.0, 41.0, 45.5 MeV, and  $46.0 \text{ MeV} \leq E_{\text{lab}} \leq 50.0 \text{ MeV}$  in 1.0 MeV steps. The cross sections were deduced by the in-beam observation of the  $\alpha$ -particles emitted in the ground state decay of the evaporation residues. The same experimental setup and technique previously [9] utilized were adopted; therefore in the following only details specific to the present experiment will be given.

Four 100  $\mu\text{m}$  thick Si detectors with 415  $\text{mm}^2$  effective surface were utilized in the following geometry:  $\pm 135^\circ$ ,  $+ 150^\circ$  at 7.0 cm from the target and  $-160^\circ$  at 10 cm from the target. The angles covered were  $\pm 9^\circ$  ( $7^\circ$ ) at 7 (10) cm. Two monitor detectors were located at  $\pm 20.0^\circ$  covering a solid angle of 0.200 msr. Two types of targets were utilized:  $\sim 190 \mu\text{gcm}^{-2}$  Bi backed by 150 (450)  $\mu\text{gcm}^{-2}$  carbon (gold). Backings were necessary to stop the evaporation residues recoils at the target site and to achieve the same geometry for the  $\alpha$  particles detection. The gold backing brings some normalization problems but had to be adopted in order to reduce as much as possible, when necessary, detectors background produced most likely from  $\beta$ -rays and light charged particles originating from the fusion of  ${}^9\text{Be}$  with the backing nuclei. The four lowest energy cross-sections from 36.0 MeV to 37.5 MeV could be measured only with the gold backing target. All the ADC's had 8k conversion dynamics so that the energy range was up to 100 MeV to allow also the observation of the  ${}^9\text{Be}$  elastic peaks.

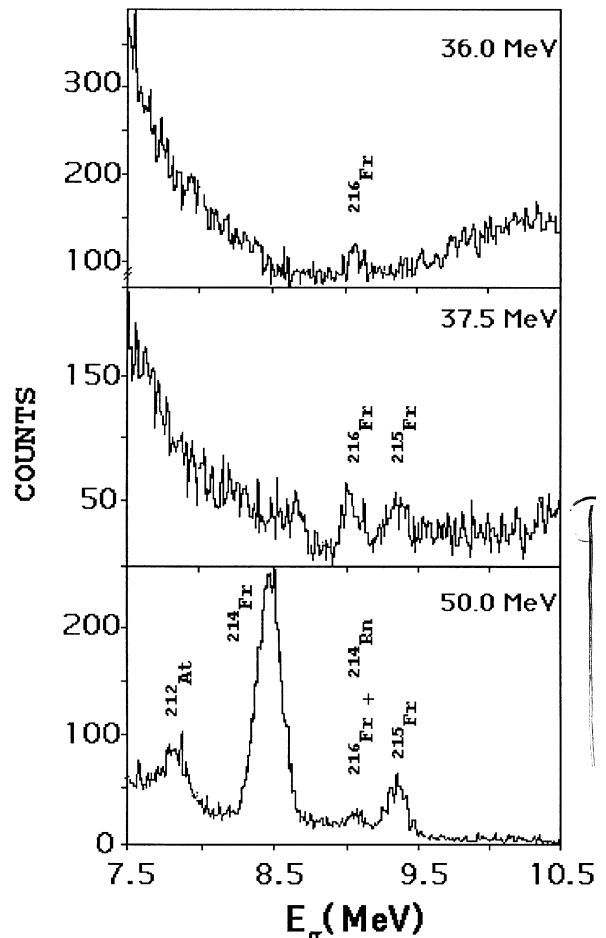


**Fig. 1.**  $\alpha$ -spectra recorded with the  $160^\circ$  detector at the lowest and highest energy and at 37.5 MeV, the lowest energy of [9]

The  $\alpha$  particles detected correspond to the decay of  ${}^{216}\text{Fr}$ ,  ${}^{215}\text{Fr}$ ,  ${}^{214}\text{Fr}$  and  ${}^{214}\text{Rn}$  populated by 2n, 3n, 4n and p3n evaporation after the fusion of  ${}^9\text{Be}$  and likely  ${}^8\text{Be}$  produced by the  ${}^9\text{Be}$  break-up. Also the fusion of  $\alpha$  and/or  ${}^5\text{He}$  particles which might originate too from the  ${}^9\text{Be}$  break-up and/or transfer processes could take place. The signatures of these processes would be the observation of  ${}^{211,212,213}\text{At}$  decays. The  ${}^{211}\text{At}$  nucleus was observed (see also [9]) but it equally originates from the  ${}^{215}\text{Fr}$  (3n evaporation)  $\alpha$ -decay.  ${}^{212}\text{At}$ ,  $E_\alpha = 7.837$  MeV, was observed at high energies while there is no evidence for  ${}^{213}\text{At}$ ,  $E_\alpha = 9.080$  MeV. No further attempt was made to quantitatively evaluate these channels since this research was focused on the complete fusion of  ${}^{8,9}\text{Be}$ . Typical examples of the  $\alpha$  spectra are shown in Fig. 1.

The absolute cross section normalization was deduced from Bi Rutherford scattering. With the Au backing the Bi peak could not be resolved from Au in the  $20^\circ$  monitor spectra. Therefore the  $20^\circ$  normalization counts  $N_{20^\circ}^{\text{Bi}}$  at the 4 lowest energies were deduced from the Au ( $N_{160^\circ}^{\text{Au}}$ ) and Bi ( $N_{160^\circ}^{\text{Bi}}$ )  $160^\circ$  scattering data and the unresolved

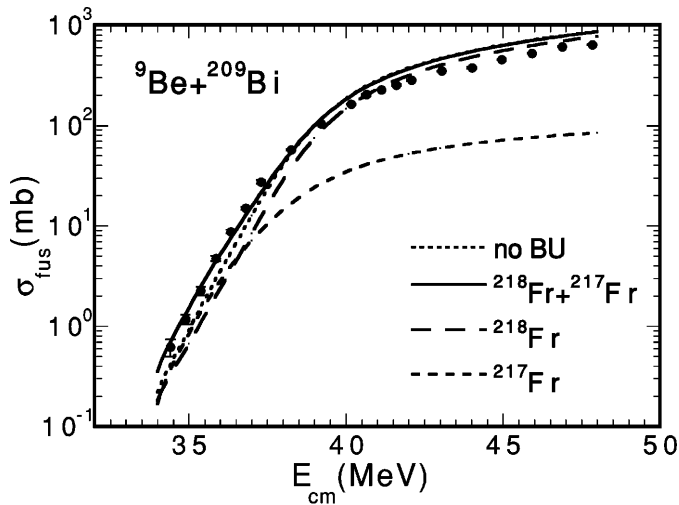


**Fig. 2.** Experimental fusion cross sections and theoretical predictions with no BU and with one BU channel (continuous line). The separate contributions from  ${}^9\text{Be}$  and  ${}^8\text{Be}$  fusion leading to  ${}^{218}\text{Fr}$  and  ${}^{217}\text{Fr}$  compound nuclei respectively are also shown

ones  $N_{20^\circ}^{\text{Au+Bi}}$  with the equation

$$\frac{N_{20^\circ}^{\text{Bi}}}{N_{160^\circ}^{\text{Bi}}} = \frac{N_{20^\circ}^{\text{Au+Bi}}}{N_{160^\circ}^{\text{Au}} + N_{160^\circ}^{\text{Bi}}}$$

valid if the elastic scattering at  $160^\circ$  behaves in the same way for Au and Bi. This can be assumed for these low energies since the absorption is very small being  $\theta_{\text{graz}} > 166.5^\circ$  for  $E_{\text{lab}} \leq 38.5$  MeV. This ratio rises slowly and smoothly with energy due to increasing absorption and was verified, as an additional normalization check, at 38.5, 40.0, 41.0 MeV (Au backing) with the cross sections previously measured [9] and at 38.0 MeV (Au and C backing data).

The complete  ${}^9\text{Be}$  plus likely  ${}^8\text{Be}$  fusion cross sections were calculated adding the  $2n+p3n$ ,  $3n$  and  $4n$  channels previously mentioned and the fission taken from [12]. The results are in agreement with [9] and consequently show the same discrepancy with [12]. For this reason the final  $\sigma_{\text{fus}}$  reported in Fig. 2 were calculated as the weighted average of the data from the present experiment and from [9]. The overall accuracy of the cross sections is  $< 5\%$  down to  $E_{\text{cm}} = 36.3$  MeV and  $< 11\%$  for the other points except the lowest at  $E_{\text{cm}} = 34.4$  MeV (20%).

In order to understand these results in the frame of current theories the data were compared with the predictions of the Dasso and Vitturi approach [6] (similar to the well known CCFUS), which explicitly takes into account the break-up process. In the calculations just one break-up channel,  ${}^9\text{Be} \rightarrow {}^8\text{Be} + n$ , was considered according to the experimental data.

To evaluate the various barrier parameters we choose a potential with the radial dependence of the Christensen and Winther one [16]. The well depth parameter  $S_0$  was adjusted to reproduce the experimental fusion excitation function of  ${}^{16}\text{O} + {}^{208}\text{Pb}$  [17] system without any additional coupling. In this system both nuclei are double

**Table 1.** Values of barrier parameters

system	$V_B$ (MeV)	$R_B$ (fm)	$\hbar\omega_B$ (MeV)	$V_{\text{cr}}$ (MeV)	$R_{\text{cr}}$ (fm)
${}^{16}\text{O} + {}^{208}\text{Pb}$	74.0	11.95	4.77	59	8.44
${}^9\text{Be} + {}^{209}\text{Bi}$	38.4	11.75	4.73	10	8.01

magic and the break-up phenomena are expected to be negligible. This is a crude approximation since a much more complex approach was developed [18] to reproduce the  ${}^{16}\text{O} + {}^{208}\text{Pb}$  fusion but it can be assumed that the first order cross section renormalization due to  ${}^{208}\text{Pb}$  and  ${}^{209}\text{Bi}$  core vibration are taken into account in this way. The well depth parameter  $S_0$  was adjusted to  $85 \text{ MeVfm}^{-1}$ , considerably lower than the standard one,  $50 \text{ MeVfm}^{-1}$ , previously adopted [9]. The parameters used in the calculations are listed in the Table 1.

The BU coupling strength parameter  $F_0$  was adjusted to 0.5 MeV in order to reproduce the subbarrier cross sections for the system  ${}^9\text{Be} + {}^{209}\text{Bi}$ . The results are shown in Fig. 2 which shows also the predictions for no BU,  $F_0 = 0$  MeV, and for the formation of  ${}^{218}\text{Fr}$  and  ${}^{217}\text{Fr}$  resulting from  ${}^9\text{Be}$  complete fusion and  ${}^8\text{Be}$  BU fusion. We have also checked the predictions of the CCFUS code with the same potential parameters and got the same results as for  $F_0 = 0$ . Below the barrier the data are well reproduced with this small BU strength which anyhow produces cross sections higher than in the no BU case. Above the barrier the theory overpredicts the experimental observations while it well reproduces the  ${}^{16}\text{O} + {}^{208}\text{Pb}$  data as shown in Fig. 3 upper panel. This is more clearly evidenced by an alternative approach utilized to interpret the "hindered" fusion cross section above the barrier of the loosely bound light systems  ${}^{6,7}\text{Li} + {}^9\text{Be}$ ,  ${}^{6,7}\text{Li} + {}^{12}\text{C}$  [13] on which discrepant higher, i.e. "no hindered", cross sections have been recently published [14]. This approach utilizes the Glas and Mosel model [19]; it is based essentially on the same theoretical grounds as [6] so should not be considered as a totally independent theory. Within this model we have compared, in the region above the barrier, the  ${}^9\text{Be} + {}^{209}\text{Bi}$  data with the  ${}^{16}\text{O} + {}^{208}\text{Pb}$  ones [17] where BU effects are to be excluded. Figure 3 shows the fusion cross sections for both systems as function of  $1/E_{\text{cm}}$ . The solid curves are the results of Dasso and Vitturi theory, already partly shown in Fig. 2. The dashed curves are the predictions of the Glas and Mosel model with the barrier parameters listed in Table 1. The critical radius  $R_{\text{cr}}$  was taken from Galin's work [20] and the potential at the critical distance  $V_{\text{cr}}$ , whose value is not critical for the calculations in this energy range, was estimated from a Woods-Saxon one. Both approaches reproduce the  ${}^{16}\text{O} + {}^{208}\text{Pb}$  system well but overestimate the  ${}^9\text{Be} + {}^{209}\text{Bi}$  experimental cross sections. There is no question that this is due to  ${}^9\text{Be}$  BU which most likely above the barrier becomes much stronger with  $\sim 25\%$  reduction of fusion cross section; consequently the Dasso and Vitturi approach with only one BU channel with constant strength fails.

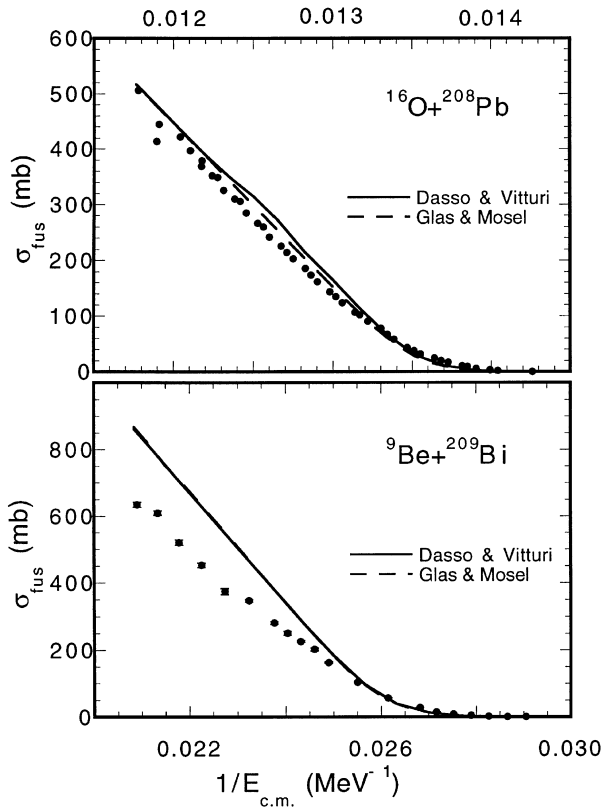


**Fig. 3.** Experimental and theoretical fusion cross sections above the Coulomb barrier. The two theories give very similar results particularly in the  ${}^9\text{Be}$  case and reproduce well the  ${}^{16}\text{O} + {}^{208}\text{Pb}$  data.

From the data we have also extracted the barrier distribution in order to see a possible signature of BU effects originating from the coupling to BU channel/s. For the experimental and theoretical fusion excitation functions the formula adopted [21] was  $D(E) = \frac{1}{\pi R^2} \frac{d^2(E\sigma_{\text{fus}})}{dE^2}$ . The second derivative was calculated using a simple point difference formula. The results are given in Fig. 4 upper panel.

Also the Rutherford elastic cross sections were measured and from these the barrier distributions were extracted according to the formula:  $D^{\text{el}}(E) = -\frac{d}{dE} \left( \frac{d\sigma_{\text{el}}}{d\sigma_{\text{R}}}(E) \right)^{\frac{1}{2}}$  [22], valid for measurements at very backward angles, ideally  $180^\circ$ . The distributions at  $150^\circ$  and  $135^\circ$  were obtained from the data recorded in this and in the previous [9] experiment. The first derivative was calculated with a point difference formula averaging over 3 consecutive points. Since the detectors were covering large angles (geometry imposed by the optimization of the fusion data) the utilization of the formula above needs some support. This is given by the positive results of a recent experiment [23] which utilized detectors located from  $156^\circ$  to  $164^\circ$ ; moreover even at  $135^\circ$  clear absorption effects were observed as confirmed by a run on elastic scattering angular distribution.

The results are shown in Fig. 4 lower panel where the predictions of optical model calculations for the same an-

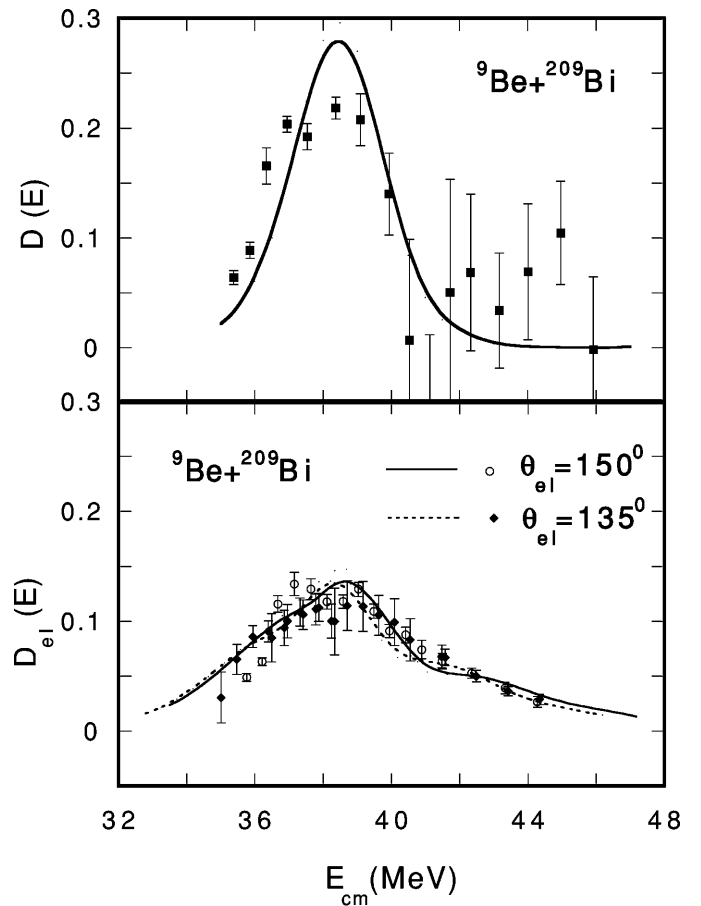


**Fig. 4.** Experimental and theoretical (continuous lines) barrier distributions (in  $\text{MeV}^{-1}$ ) from fusion data, top panel, and from elastic scattering data, bottom panel

gular acceptance are also presented. These calculations were done with the code PTOLEMY utilizing a Woods-Saxon potential with parameters deduced from an elastic scattering measurement. All distributions are automatically normalized to 1 therefore the same y-scale was utilized in Fig. 4 for a better comparison.

All barrier distributions of Fig. 4 present basically one peak structure narrower for the fusion data than for the elastic scattering ones. There is no evident signature of BU effects in these data; it is essentially only one barrier which regulates the fusion process.

The fact that from the elastic scattering data a broader barrier distribution is deduced from both detectors could be very tentatively interpreted as due to the  $\alpha$ -BU channels which can influence only the scattering data and not the fusion ones, sensitive only to n-BU channel. This effect could be identified in the small sidebumps of the theoretical curves, where experimentally deduced potential parameters were used, but are too small to be evidenced with the present experimental setup; a more focused experiment is necessary for this purpose.

By the completion of this paper the results of a similar work on  ${}^9\text{Be} + {}^{208}\text{Pb}$  [24] were kindly communicated to us. In this work in addition to  ${}^9\text{Be}$  fusion also a significant in-

complete fusion component, assigned to  $\alpha$  BU, is reported. Their coupled channel calculations can reproduce the fusion + incomplete fusion data above the barrier but not below while the complete fusion only is reproduced scaling the previous calculations by a factor of 0.68. This implies a reduction in fusion strength of around  $\sim 30\%$  similar to our value. The barrier distribution deduced from the fusion data is very similar to our. Essentially both works point out to very similar conclusions.

In summary from the  ${}^9\text{Be} + {}^{209}\text{Bi}$  fusion cross sections, compared to the  ${}^{16}\text{O} + {}^{208}\text{Pb}$  ones, there is no strong influence of BU effects below the barrier and the data are well reproduced including only one BU channel with moderate strength. Above the barrier the  ${}^9\text{Be}$  data suggest a consistent BU effect as opposed to  ${}^{16}\text{O} + {}^{208}\text{Pb}$  ones. All the barrier distributions show the presence of essentially one barrier more or less broad; this is interpreted as a lack of additional signature of BU effects.

We thank the staff of the Munich Tandem, especially W. Carli, for their professional operation of the accelerator and to H.J. Maier from the Technological Laboratory of the University of Munich and his staff for the target preparation.

## References

1. K. Riisager et al., Nucl. Phys. **A540**, (1992) 365
2. B. Blank et al., Nucl. Phys. **A555**, (1993) 408
3. T. Kobayashi, Phys. Lett. **B232**, (1989) 51
4. C.H. Dasso, J.L. Guisado, S.M. Lenzi, A. Vitturi, Nucl. Phys. **A597**, (1996) 473
5. L.F. Canto, R. Donangelo, M.S. Hussein, M.P. Pato, Nucl. Phys. **A542**, (1992) 131
6. C.H. Dasso, A. Vitturi, Phys. Rev. **C50** (1994) R12
7. M.S. Hussein, M.P. Pato, L.F. Canto, R. Donangelo, Phys. Rev. **C46**, (1992) 377 and Phys. Rev. **C47**, (1993) 2398
8. N. Takigawa, M. Kuratani, H. Sagawa, Phys. Rev. **C47**, (1993) R2470
9. C. Signorini et al., Eur. Phys. J. **A2**, (1998) 227
10. K.E. Rehm et al., Phys. Rev. Lett. **81**, (1998) 3341
11. V. Fekou-Youmbi et al., Nucl.Phys. **A583**, (1995) 811c
12. A. Yoshida et al., Phys. Lett. **B389**, (1996) 457
13. J. Takahashi et al., Phys. Rev. Lett. **78**, (1997) 30
14. A. Mukherjee et al., Nucl. Phys. **A635**, (1998) 305
15. F. Soramel et al., *Proceeding of 3<sup>rd</sup> Japan-Italy Joint Symposium '97, Padova, Italy, October 1997*, eds. C. Signorini, F. Soramel, T. Kishida (World Scientific, Singapore 1999) 83
16. P.R. Christensen, A. Winther, Phys. Lett. **B65**, (1976) 19
17. C.R. Morton et al., Phys. Rev. **C52**, (1995) 243
18. I.J. Thompson, M.A. Nagarajan, J.S. Lilley, M.J. Smithson, Nucl. Phys. **A505**, (1989) 84
19. D. Glas, U. Mosel, Nucl. Phys. **A237**, (1975) 429
20. J. Galin, D. Guerreau, M. Lefort, X. Tarrago, Phys. Rev. **C9**, (1974) 1018
21. N. Rowley, G.R. Satchler, P.H. Stelson, Phys. Lett. **B254**, (1991) 25 and J.R. Leigh et al., Phys. Rev. **C52**, (1995) 3151
22. N. Rowley et al., Phys. Lett. **B373**, (1996) 23
23. H.Q. Zhang et al., Phys. Rev. **C57**, (1998) R1047
24. M. Dasgupta et al., Phys. Rev. Lett. **82**, (1999) 1395